

## Preparation and Properties of Fe-Substituted $V_6O_{13}$

M. GREENBLATT,\* D. W. MURPHY, F. J. DISALVO, M. EIBSCHUTZ,  
S. M. ZAHURAK, AND J. V. WASZCZAK

*Bell Laboratories, Murray Hill, New Jersey 07974*

Received October 23, 1981; in final form January 8, 1982

Iron-substituted  $V_6O_{13}$  with the maximum iron composition of  $Fe_{0.5}V_{5.5}O_{13}$  was prepared. Single-crystal electrical resistivity, Mössbauer spectra, and magnetic susceptibility are reported.

### Introduction

Recent interest in lithium insertion compounds of  $V_6O_{13}$  (1-3) and in the metal-insulator transition in  $V_6O_{13}$  (4-5) has led us to study iron-substituted compositions  $Fe_xV_{6-x}O_{13}$ . The existence of  $FeV_3O_8$  (6), which has the monoclinic  $VO_2(B)$ , structure, and the close structural relationship between  $V_6O_{13}$  and  $VO_2(B)$  (7, 8) suggested that substantial iron substitution in  $V_6O_{13}$  might be possible. The lithium insertion product  $Li_2FeV_3O_8$  (9) exhibited improved crystallinity over the unsubstituted  $Li_xVO_2(B)$ , allowing a detailed refinement of the  $Li_2FeV_3O_8$  structure by neutron diffraction powder profile analysis (NDPPA) (10). The fully lithiated  $Li_8V_6O_{13}$  is poorly crystalline, hence it was not possible to carry out NDPPA. It was hoped that a similar improvement in the crystallinity of the fully lithiated Fe-substituted  $V_6O_{13}$  might be achieved to allow the NDPPA.

The unsubstituted  $V_6O_{13}$  is a "borderline" metal at room temperature and undergoes a metal-to-insulator transition at 147°K

(4). The magnetic signature of this transition is eliminated by insertion of as little as 0.03 Li/V. Thus, the influence of Fe substitution on electron localization in  $V_6O_{13}$  is also of interest.

### Experimental

Polycrystalline samples with the composition  $Fe_{0.5}V_{5.5}O_{13}$  were prepared by heating stoichiometric mixtures of  $Fe_2O_3$ ,  $V_2O_5$ , and V in evacuated quartz ampoules at 500°C overnight, then increasing the temperature to 650°C for 1 to 2 days. Similar methods were used to prepare  $Fe_xV_{6-x}O_{13}$  ( $0.12 < x \leq 0.5$ ) from stoichiometric mixtures of  $Fe_{0.5}V_{5.5}O_{13}$  and  $V_6O_{13}$ . Single crystals of  $Fe_{0.5}V_{5.5}O_{13}$  and  $Fe_{0.17}V_{5.83}O_{13}$  were grown by vapor transport in evacuated quartz tubes with  $TeCl_4$  as the transport agent.  $T_1 = 600^\circ C$  at the charge zone and  $T_2 = 550^\circ C$  at the growth zone were used. After 1 week of transport, very thin black platelet crystals ( $\sim 0.5 \times 0.2 \times 0.01$  cm) were obtained in each case. The X-ray diffraction pattern of pulverized crystals showed a single phase similar to  $V_6O_{13}$  with slightly shifted  $d$  values. X-Ray milliprobe analysis of the crystals indicated that they

\* Work performed while on sabbatical leave from the Chemistry Department, Rutgers University, New Brunswick, N.J. 08903.

had a uniform composition of  $Fe_{0.5}V_{5.5}O_{13}$  and  $Fe_{0.17}V_{5.83}O_{13}$ , respectively. We have confirmed the X-ray milliprobe results by quantitative chemical analysis (11) of the vanadium and iron contents of pulverized crystal samples.

Powder X-ray diffraction patterns of all phases were obtained on a G.E. diffractometer with  $CuK\alpha$  radiation. Magnetic susceptibility data were obtained by the Faraday method on powder samples sealed in quartz tubes. Four-probe dc conductivity measurements were made on single crystals of  $Fe_{0.5}V_{5.5}O_{13}$  and  $Fe_{0.17}V_{5.83}O_{13}$  which were oriented by the X-ray precession method. The  $^{57}Fe$  Mössbauer spectra of  $Fe_{0.5}V_{5.5}O_{13}$  were obtained in a standard transmission geometry with a conventional constant acceleration spectrometer using a  $^{57}Co$  in Pd source. Powder absorbers for Mössbauer effect measurements were made in dry helium atmospheres by mixing the material with boron nitride.

## Results and Discussion

The  $V_6O_{13}$  structure may be visualized as arising from a (3,2) shear of the cubic  $ReO_3$  type (7, 8). Similarly,  $V_2O_5$  and  $VO_2(B)$  may be viewed as (2, $\infty$ ) and (2,2) shear structures of the same family. The  $VO_2(B)$  structure consists of edge-shared, double zig-zag chains joined by corner-sharing oxygens (Fig. 1). The idealized  $V_2O_5$  structure consists of corner-shared single zig-zag chains. Finally,  $V_6O_{13}$  has alternating single and double chains and may be thought of as an interleaving of the two structures, " $V_2O_5 \cdot 4VO_2(B)$ ." Thus, since the double chain portion of  $V_6O_{13}$  is so similar to  $VO_2(B)$  we expected " $V_2O_5 \cdot FeV_3O_8$ " or  $FeV_5O_{13}$  to be a reasonable stoichiometry for Fe substitution in  $V_6O_{13}$ . However, at this stoichiometry we were unable to pre-

### DERIVATION OF SOME $ReO_3$ SHEAR STRUCTURES

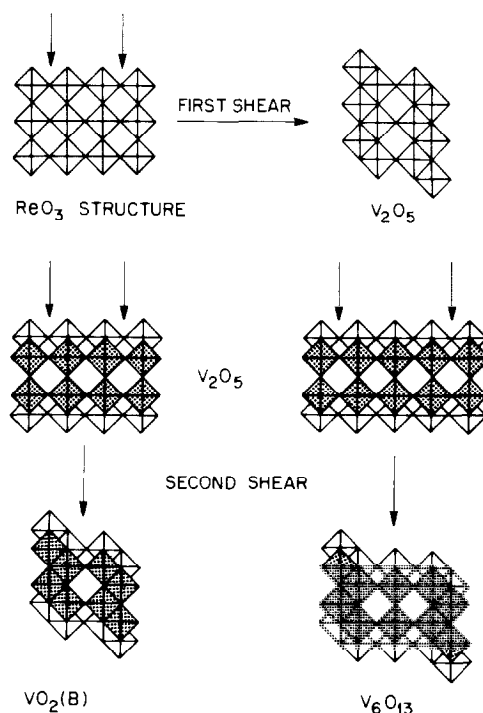


FIG. 1. The idealized  $V_2O_5$  lattice is derived by a shear of the  $ReO_3$  lattice along the planes indicated by arrows. The  $VO_2(B)$  and  $V_6O_{13}$  lattices are derived by a shear of the  $V_2O_5$  lattice as indicated.

pare single-phase products; additional lines always appeared along with a  $V_6O_{13}$ -like X-ray pattern with slightly shifted lattice parameters. Subsequently, vapor transport with  $TeCl_4$  of the impure " $FeV_5O_{13}$ " yielded crystals of composition as high as  $Fe_{0.5}V_{5.5}O_{13}$  as determined by chemical analysis. Homogeneous polycrystalline powder samples were then prepared with this maximum Fe stoichiometry.

The monoclinic unit cell parameters of  $Fe_{0.5}V_{5.5}O_{13}$ ,  $a = 11.976 \text{ \AA}$ ,  $b = 3.683 \text{ \AA}$ ,  $c = 10.206 \text{ \AA}$ , and  $\beta = 101.27^\circ$ , were obtained by least-squares refinement of 14 strong X-ray diffraction peaks. (The cell parameters of  $V_6O_{13}$  are:  $a = 11.922 \text{ \AA}$ ,  $b = 3.680 \text{ \AA}$ ,  $c = 10.138 \text{ \AA}$ , and  $\beta = 100.87^\circ$ ).

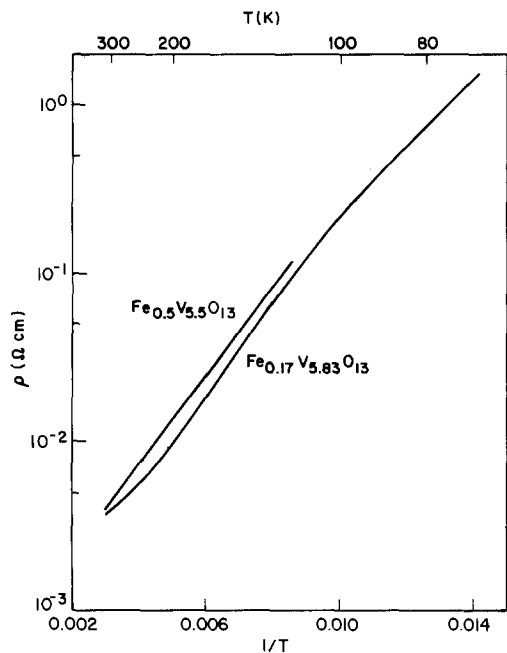


FIG. 2. Resistivity vs  $1/T$  of  $\text{Fe}_{0.5}\text{V}_{5.5}\text{O}_{13}$  and  $\text{Fe}_{0.17}\text{V}_{5.83}\text{O}_{13}$ .

The electrical resistivity was measured on crystals of composition  $\text{Fe}_{0.5}\text{V}_{5.5}\text{O}_{13}$  and  $\text{Fe}_{0.17}\text{V}_{5.83}\text{O}_{13}$  along the unique direction. Both compositions are semiconducting (Fig. 2).  $\text{Fe}_{0.5}\text{V}_{5.5}\text{O}_{13}$  has  $\rho(300 \text{ K}) \approx (5 \pm 1) \times 10^{-3} \Omega \text{ cm}$  and fits a simple exponential form  $\rho = \rho_0 e^{T_0/T}$  between 300–80 K with an activation energy of approximately 0.05 eV. The data for  $\text{Fe}_{0.17}\text{V}_{5.83}\text{O}_{13}$ , however, do not fit a simple exponential over a significant temperature interval in the temperature range of measurement. The similar magnitude of its resistivity and slope to that of  $\text{Fe}_{0.5}\text{V}_{5.5}\text{O}_{13}$  shows that the “effective” activation energy is similar to that of  $\text{Fe}_{0.5}\text{V}_{5.5}\text{O}_{13}$ . The semiconducting-like behavior of both compounds may be due to Mott localization, with the small activation energies due to defect or impurity levels close to the band edges. An alternative explanation is that the carriers become localized due to the random Fe substitution (Anderson localization) (12) with the activa-

tion energy being given by the difference between the Fermi energy and the mobility edge.

The  $^{57}\text{Fe}$  Mössbauer effect was used to study the electronic spin configuration of Fe in  $\text{Fe}_{0.5}\text{V}_{5.5}\text{O}_{13}$ . The room temperature and 4.2 K Mössbauer absorption spectra for  $\text{Fe}_{0.5}\text{V}_{5.5}\text{O}_{13}$  are given in Figs. 3a,b.

The room temperature spectrum shows two resonance lines due to quadrupole splitting; the asymmetry in line intensity of the spectrum is due to preferred orientation of crystallites in the powder sample. The spectrum was analyzed by fitting to the sum of two Lorentzian curves of independent position, width, and depth. The quadrupole splitting is  $\frac{1}{2}e^2qQ[1 + (\eta^2/3)]^{1/2} = 0.79 \pm 0.01 \text{ mm/sec}$ . The linewidths of the two peaks are broad,  $\text{FWHM} = 0.35 \pm 0.01 \text{ mm/sec}$  ( $\text{FWHM} = \text{full width at half-maximum}$ ), indicating a distribution of quadrupole splittings which might be due to small variations in the site symmetry of the Fe ions and/or to the differences in the oxidation states of the nearest-neighbor vanadium ions at a given Fe site. The three

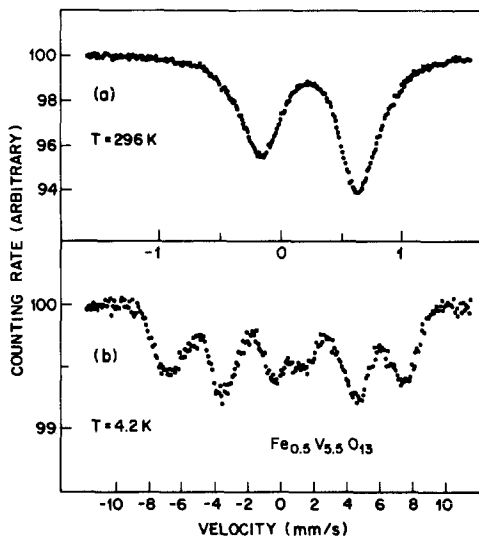


FIG. 3. Mössbauer spectrum of  $\text{Fe}_{0.5}\text{V}_{5.5}\text{O}_{13}$  at room temperature and at 4.2 K. Upper scale refers to room temperature, lower scale to 4.2-K data.

crystallographically unique sites for (Fe, V) present in the  $Fe_{0.5}V_{5.5}O_{13}$  structure are not resolved in the room temperature spectrum because of the broad distribution of quadrupole splittings at each Fe site. The isomer shift of  $0.42 \pm 0.01$  mm/sec with respect to Fe metal indicates that iron is in the  $Fe^{3+}$  spin state.

At 4.2 K the Mössbauer spectrum shows a hyperfine splitting with rather broad FWHM ( $\approx 1$  mm/sec) and complex absorption lines, indicating a distribution of hyperfine fields. At least three hyperfine fields are evident:  $H_{hf}(1) = 448 \pm 10$  kOe,  $H_{hf}(2) = 400 \pm 10$  kOe, and  $H_{hf}(3) = 350 \pm 10$  kOe. These  $H_{hf}$  results suggest that the Fe ions are randomly distributed on the three crystallographically nonequivalent sites, and that the electronic environment around the iron in each of these sites is slightly different. The similar isomer shifts  $IS = 0.64 \pm 0.05$  mm/sec with respect to Fe metal for each Fe site indicate that all of the  $Fe^{3+}$  is in the high spin state (in agreement with the susceptibility results below).

Since the electrical measurements indicate that the electrons are localized, oxidation states may be assigned to each transition metal:  $Fe_{0.5}^{3+}V_{2.5}^{5+}V_3^{4+}O_{13}$ .

Results of the magnetic susceptibility measurement of  $Fe_{0.5}V_{5.5}O_{13}$  powder sample

between 300–4.2 K are shown in Fig. 4. No magnetic signature of the metal–insulator transition characteristic of  $V_6O_{13}$  ( $\approx 147$  K) or  $VO_2$  ( $\approx 342$  K) is observed in the Fe-substituted  $V_6O_{13}$ . The susceptibility does not fit the Curie–Weiss law over a broad temperature range, but in the region 100–360 K a reasonable fit is obtained with  $\theta \sim 80 \pm 30$  K and  $C_M \sim 3.05$  emu-K/mole. The observed value of  $\chi_g(300\text{ K}) = 15.6 \times 10^{-6}$  emu/g is about twice the magnitude of the susceptibility of  $V_6O_{13}$  ( $\chi_g(300\text{ K}) = 7.4 \times 10^{-6}$  emu/g), indicating that Fe is in the high spin state. For high-spin  $Fe^{3+}$  we expect the contribution for the Curie constant per mole of Fe to be  $C_M = \mu_{eff}^2/8 = (\frac{5}{2})g^2S(S+1) = 4.4$ ; the  $V^{4+}$  ions in  $Fe_{0.5}V_{5.5}O_{13}$  with  $S = \frac{1}{2}$  each contribute  $C_M = 0.375$ , assuming  $g = 2$  in both cases. The observed  $C_M \sim 3.05$  accounts fairly well for what is expected on the basis of localized spins in the compound (i.e.,  $\frac{1}{2} \times 4.4 + 3 \times 0.375$ ). Below 10 K the susceptibility appears to saturate, suggesting some antiferromagnetic “order” at low temperatures, perhaps of the spin glass type (13). This suggestion is further supported by the low-temperature Mössbauer measurements which indicate the presence of large hyperfine fields at 4.2 K.

No change in the magnetic susceptibility of  $Fe_{0.17}V_{5.83}O_{13}$  powder sample is observed after two firings at  $650^\circ\text{C}$ , suggesting that the equilibrium composition has been reached. In this sample the concentration of unreacted  $V_6O_{13}$  is very small, as evidenced by a barely visible transition at the temperature expected for  $V_6O_{13}$ . The  $\chi_g$  vs  $T$  curve is similar in shape (Fig. 4) to that of  $Fe_{0.5}V_{5.5}O_{13}$ ; however,  $\chi_g$  could not be fit to the Curie–Weiss law over the temperature range of measurement due to the small  $V_6O_{13}$  impurity.

The magnetic susceptibility of a polycrystalline sample of nominal composition  $Fe_{0.1}V_{5.9}O_{13}$  versus temperature, shown in Fig. 5, is qualitatively similar to that of

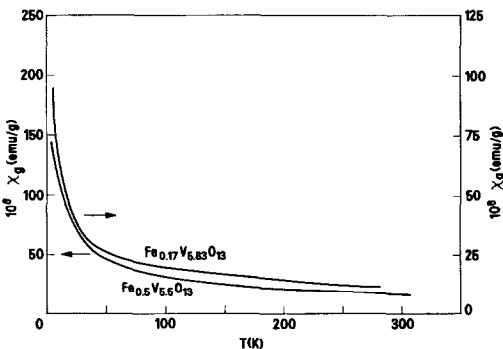


FIG. 4. Magnetic susceptibility vs  $T$  of  $Fe_{0.5}V_{5.5}O_{13}$  and  $Fe_{0.17}V_{5.83}O_{13}$ .

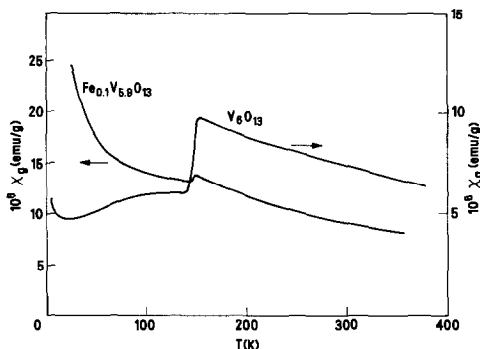


FIG. 5. Magnetic susceptibility vs  $T$  of  $\text{Fe}_{0.1}\text{V}_{5.9}\text{O}_{13}$  and  $\text{V}_6\text{O}_{13}$ .

$\text{Fe}_{0.5}\text{V}_{5.5}\text{O}_{13}$  except for the transition at 147 K, indicating the presence of about 20%  $\text{V}_6\text{O}_{13}$  second phase. The amount of this second phase does not decrease after repeated firings at  $650^\circ\text{C}$ . The continued presence of the  $\text{V}_6\text{O}_{13}$  impurity suggests that  $\text{Fe}_x\text{V}_{6-x}\text{O}_{13}$  is homogeneous only over the range  $0.12 < x \leq 0.5$  at  $650^\circ\text{C}$ .

Treatment of  $\text{Fe}_{0.5}\text{V}_{5.5}\text{O}_{13}$  with a dilute solution of  $n\text{-BuLi}$  in hexane at room temperature results in  $\text{Li}_x\text{Fe}_{0.5}\text{V}_{5.5}\text{O}_{13}$  with a maximum of  $x = 5.5$ . This stoichiometry is comparable to that obtained with non-stoichiometric  $\text{V}_6\text{O}_{13+x}$  (3). However, the X-ray pattern shows broadened lines and these samples are therefore unsuitable for NDPPA.

## Conclusion

Iron may be substituted for vanadium in  $\text{V}_6\text{O}_{13}$ , but only to about one-half the extent suggested by a structural analogy with  $\text{VO}_2(B)$ . Single crystals may be grown by vapor transport with  $\text{TeCl}_4$ . Mössbauer results suggest that iron is randomly substi-

tuted on all three crystallographic sites. These measurements, as well as magnetic susceptibility, show that Fe is present as high-spin  $\text{Fe}^{3+}$ .

The crystals are semiconducting, probably due to Mott or Anderson localization; thus, the low-temperature metal-insulator transition is no longer possible.

## References

1. K.-A. WILHELM, K. WALTERSSON, AND L. KIHLEBORG, *Acta Chem. Scand.* **25**, 2675 (1971).
2. D. W. MURPHY, P. A. CHRISTIAN, J. N. CARIDES, AND F. J. DISALVO, in "Fast Ion Transport in Solids" (P. Vashishta, J. N. Mundy, and G. K. Shenoy, Eds.), p. 137 North-Holland, New York, (1979).
3. D. W. MURPHY, P. A. CHRISTIAN, F. J. DISALVO, AND J. N. CARIDES, *J. Electrochem. Soc.* **126**, 497 (1979); D. W. MURPHY, P. A. CHRISTIAN, F. J. DISALVO, J. N. CARIDES, AND J. V. WASZCZAK, *J. Electrochem. Soc.* **128**, 2053 (1981).
4. S. KACHI, K. KOSUGE, AND H. OKINAKA, *J. Solid State Chem.* **6**, 258 (1973).
5. A. C. GOSSARD, F. J. DISALVA, L. C. ERICH, J. P. REMEIK, AND H. YASUOKA, *Phys. Rev. B* **10**, 4178 (1974).
6. J. MULLER, J. C. JOUBERT, AND M. MAREZIO, *J. Solid State Chem.* **27**, 191 (1979).
7. K. KAWASHIMA, K. KOSUGE, AND S. KACHI, *Chem. Lett.*, 1131 (1975).
8. S. ANDERSON, *Bull. Soc. Chim. Fr.*, 1088 (1965).
9. D. W. MURPHY, M. GREENBLATT, R. J. CAVA, AND S. M. ZAHURAK, *Solid State Ionics* **5**, 3 (1981).
10. R. J. CAVA, D. W. MURPHY, A. J. SANTORO, R. S. ROTH, AND S. M. ZAHURAK, *Solid State Ionics* **5**, 323 (1981).
11. C. L. WILSON AND D. W. WILSON, Eds., "Comprehensive Analytical Chemistry," pp. 547-646, Elsevier, Amsterdam (1962).
12. N. F. MOTT, M. PEPPER, S. POLLITT, R. H. WALLIS, AND C. J. ADKINS, *Proc. Roy. Soc. London Ser. A* **345**, 169 (1975).
13. J. J. HAUSER AND J. V. WASZCZAK, *Phys. Rev. B* **18**, 6206 (1978).